

ELECTRONIC SUPPLEMENTARY INFORMATION

MOF-polymer enhanced compatibility: post-annealed zeolite imidazolate framework membranes inside polyimide hollow fibers

Fernando Cacho-Bailo,^a Guillermo Caro,^a Miren Etxeberria-Benavides,^b Oğuz Karvan,^b Carlos Téllez,^a Joaquín Coronas^{a,}*

^a Chemical and Environmental Engineering Department and Instituto de Nanociencia de Aragón (INA), Universidad de Zaragoza, 50018 Zaragoza, Spain

^b TecNALIA Research and Innovation, Energy and Environmental Division, 20009 Donostia-San Sebastián, Spain

P84 hollow fiber fabrication procedure. HFs with an asymmetric morphology were spun using the dry jet, wet quench method.¹ Through a spinning process, a polymer solution (polymer, solvents, non-solvents, additives) was co-extruded with the bore fluid (a solvent-rich mixture of solvent and non-solvent) through a spinneret. When the extruded solution passed through the air gap, a skin layer formed due to the vaporization of the solvent with a high vapor pressure. Then the fiber reached the quench bath and a rapid phase separation occurred. A porous substructure was formed while the fiber travelled through the quench bath. After the quench bath, the fiber was wound onto a take-up drum and kept in the drum for further rinsing for 15-20 min. The fibers were removed from the drum, kept in DI water for four days for cleaning. Then they were solvent exchanged by means of three 30 min successive methanol baths followed by three 30 min hexane baths.² The last solvent (hexane) was removed by drying at 70 °C under vacuum overnight. The dope composition and fiber spinning conditions used in this work are shown in Table S1, comprising NMP (anhydrous N-methylpyrrolidone, Sigma-Aldrich, 99.5%) and EtOH (anhydrous ethanol, Prolabo). Co-polyimide P84 was generously supplied by HP Polymer GmbH. The parameters of the spinning process are given in Table S2. Additional details regarding the spinning process and principles can be found elsewhere.^{2,3}

ZIF@P84 membrane fabrication procedure. ZIF-8 membranes were prepared mixing a $0.1 \text{ mol}\cdot\text{L}^{-1}$ $\text{Zn}(\text{NO}_3)_2\cdot6\text{H}_2\text{O}$ (Sigma Aldrich, 98%) solution with a $0.3 \text{ mol}\cdot\text{L}^{-1}$ 2-N-methylimidazole (Sigma Aldrich, 99%) and sodium formate (NaCOOH, Sigma Aldrich, >99%) solution in methanol (Scharlab, 99.9%) at room temperature. The syntheses lasted 2.5 h, the final volume pumped through the hollow fiber being 15 mL. Finally, 2 mL of methanol were pumped for washing.

For the fabrication of ZIF-93 membranes (ZIF-93@P84), a $0.15 \text{ mol}\cdot\text{L}^{-1}$ zinc nitrate hexahydrate solution ($\text{Zn}(\text{NO}_3)_2\cdot6\text{H}_2\text{O}$, Sigma-Aldrich, 98%) in water was mixed together with a $0.30 \text{ mol}\cdot\text{L}^{-1}$ 4-methyl-5-imidazolecarboxaldehyde ($\text{C}_5\text{H}_6\text{N}_2\text{O}$, Sigma-Aldrich, 99%) and $0.30 \text{ mol}\cdot\text{L}^{-1}$ sodium formate (NaCOOH, Sigma-Aldrich, >99%) solution in methanol (Scharlab, 99.9%) as metal and ligand solutions, respectively.

The ZIF-93 membrane syntheses lasted 80 min at a total flow rate of 50 μ L/min, a total volume of 4 mL of the reagent solution being pumped. Finally, 2 mL of a distilled water were pumped for washing.

These conditions gave rise to a laminar flow within the P84 HF: dissolved reagent transfer was enhanced through the boundary layers towards the HF wall. A residence time (τ) of 7.7 s was calculated for the flow inside the fiber.

Table S1. Composition of the dope and the bore solutions used in the P84 HF spinning process.

	Polymer solution [wt%]	Bore fluid [wt%]
P84 (HP Polymer GmbH)	28.5	-
NMP	62.4	89.9
DI water	-	10.1
EtOH	9.1	-

Table S2. Working conditions used in the P84 HF spinning process.

Dope flow	Dope pressure	Bore flow	Bore fluid pressure	Spinneret temp.	Quench bath temp.	Air gap	Take up rate	Room temp.	Humidity
[mL/h]	[atm]	[mL/h]	[atm]	[$^{\circ}$ C]	[$^{\circ}$ C]	[cm]	[m/min]	[$^{\circ}$ C]	[%]
180	10.9	60	0.1	35	25	10	25	24	69

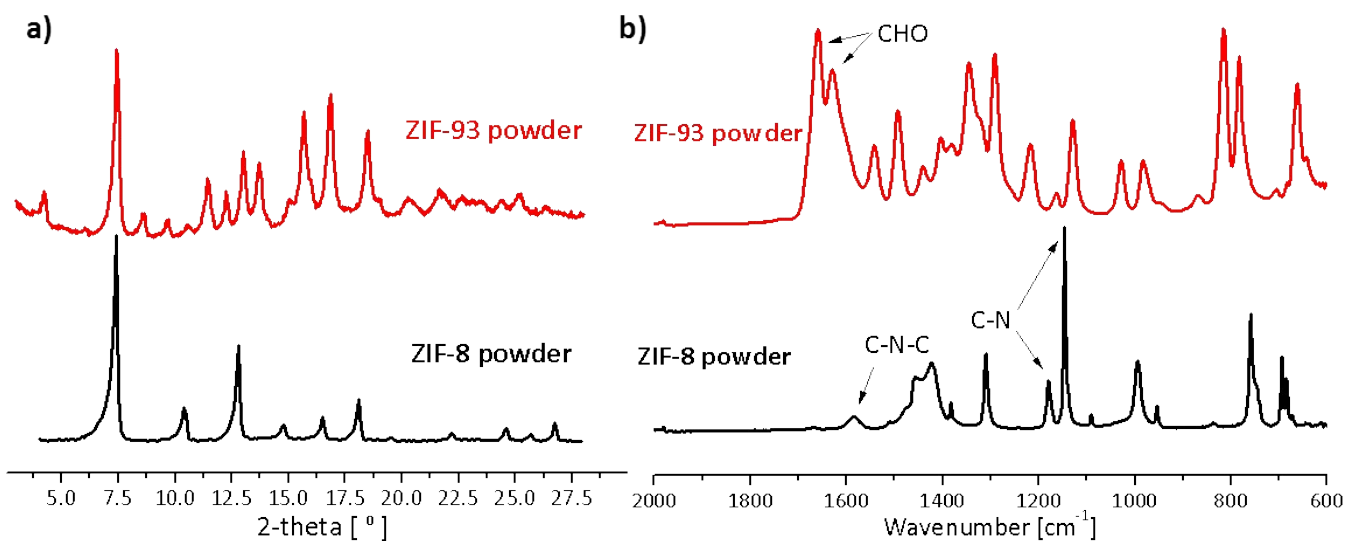


Figure S1. XRD (a) and FTIR (b) patterns of the ZIF-8 and ZIF-93 powders collected during the membrane syntheses and XRD pattern of a dissolved ZIF-93@P84 membrane.

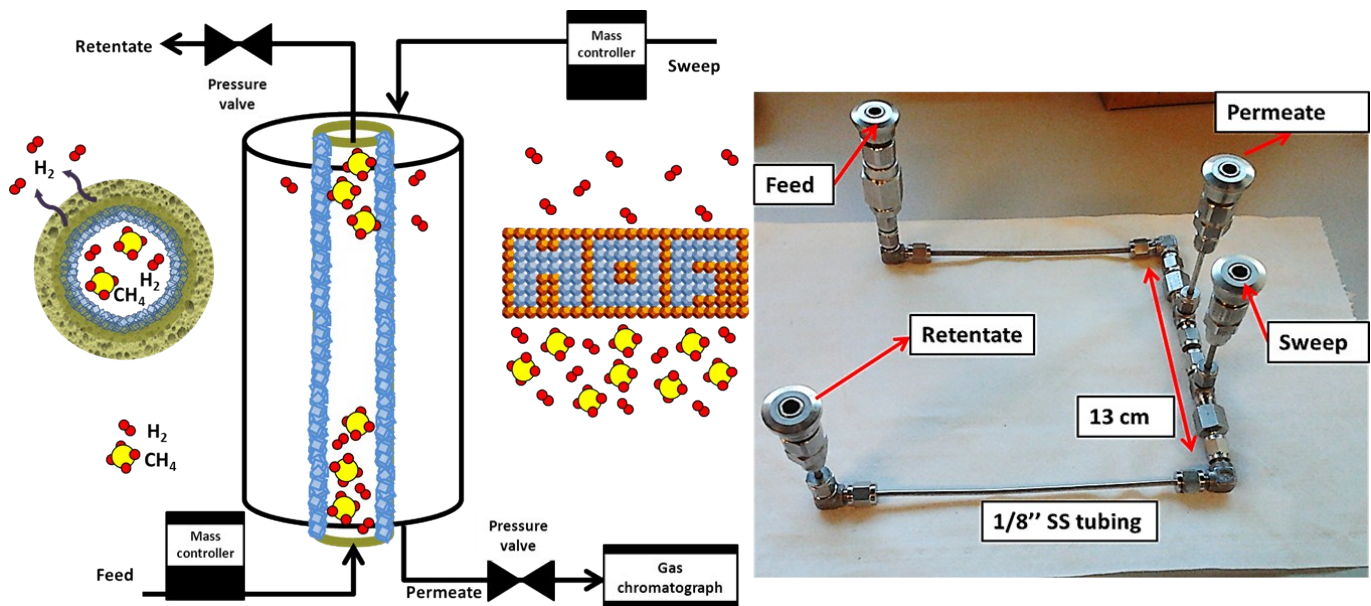


Figure S2. Gas plant scheme and experimental stainless-steel module used for HF membrane permeation tests. A 13 cm long HF is sealed with epoxy resin where an equimolar gas mixture to be separated is fed inside the fiber. The permeate stream is swept crosscurrent.

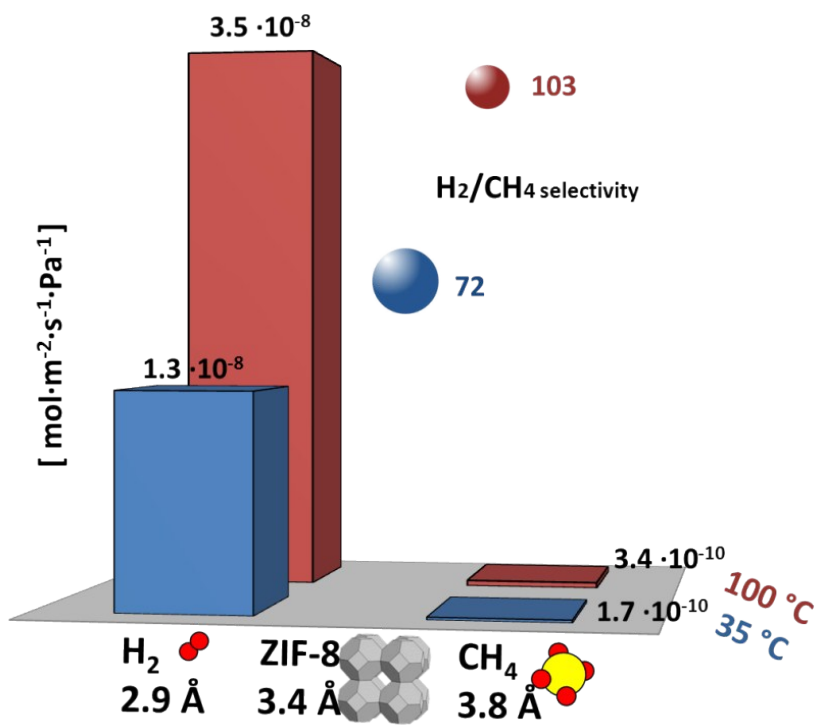


Figure S3. Averaged performance values of an *in situ* annealed ZIF-8@P84 HF membrane in H_2/CH_4 mixture separation at 35 and 100 $^\circ\text{C}$. Dots represent the mixture selectivities, whereas bars are permeances.

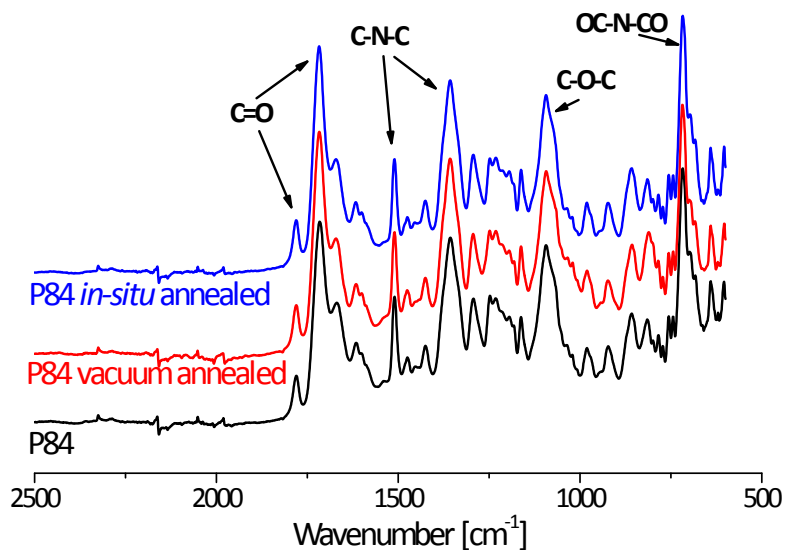


Figure S4. ATR-FTIR spectra of the *in situ* (B-type membrane) and vacuum (C-type membrane) annealed P84 HF supports compared with the bare P84 polymer (A-type membrane) support.

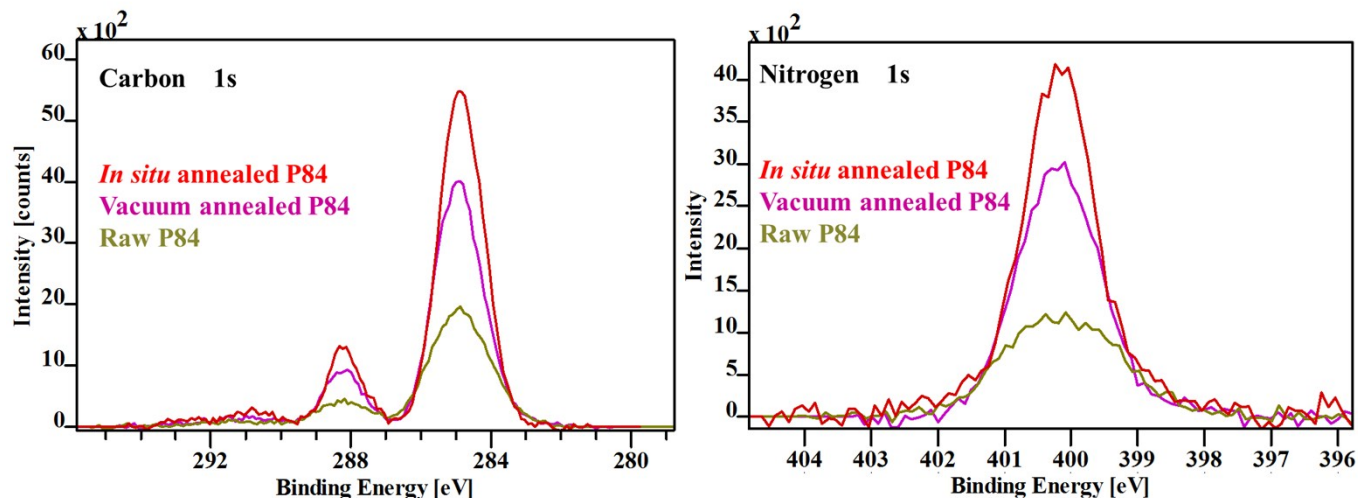


Figure S5. Carbon (1s) and nitrogen (1s) high resolution XPS spectra of the inner-surface of bare (A-type), vacuum annealed (C-type) and *in situ* annealed (B-type membrane) P84 HF supports.

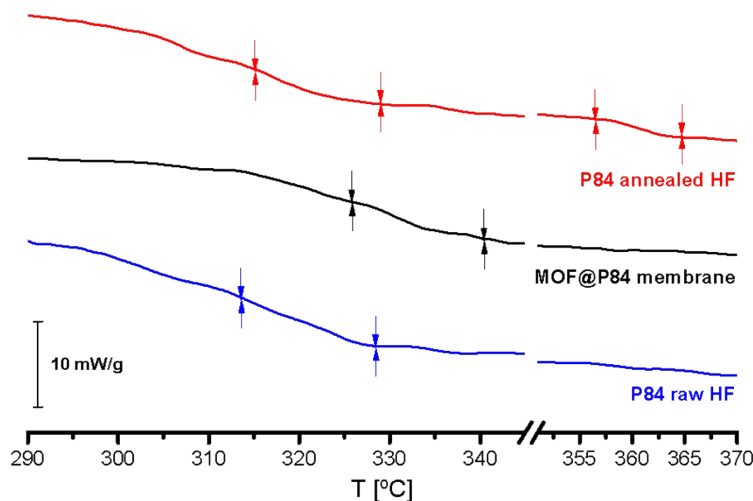


Figure S6. DSC curves of a MOF coated, raw and annealed P84 hollow fiber membranes carried out at $5\text{ K}\cdot\text{min}^{-1}$. Inflection regions showing the glass transition temperatures of the polymeric materials are indicated.

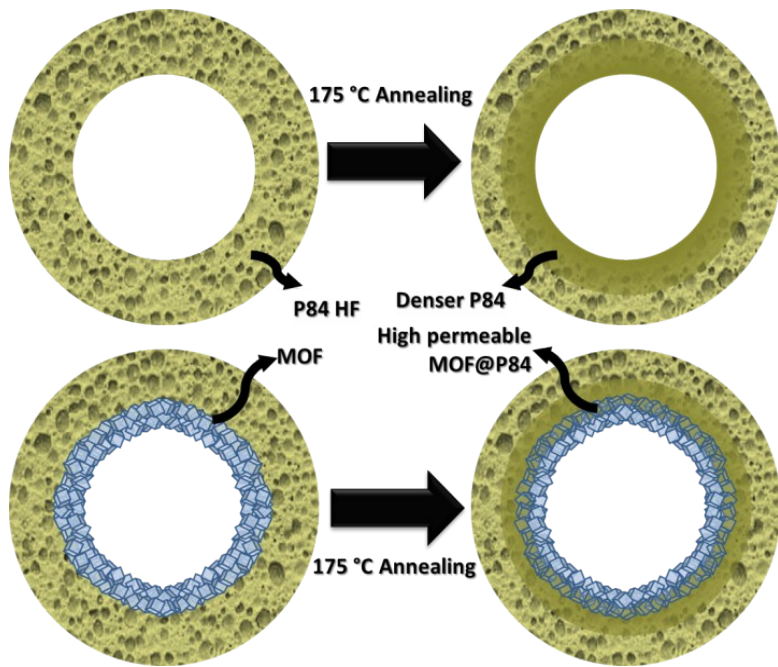


Figure S7. MOF-membrane schematic composition and hypothesized changes induced by the annealing treatment.

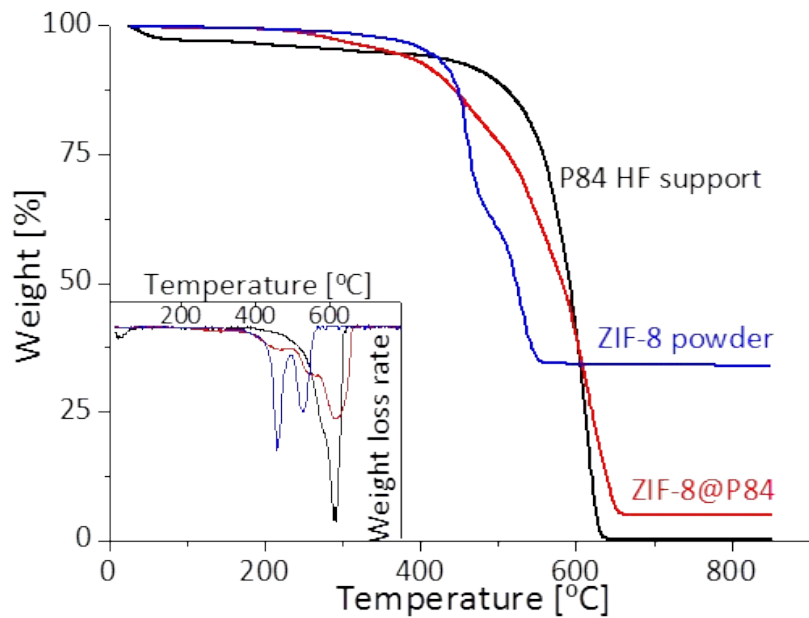


Figure S8. Weight loss curves in air atmosphere of ZIF-8 *in situ* annealed (G-type) membrane, compared with the pure P84 hollow fiber support and the collected MOF powder.

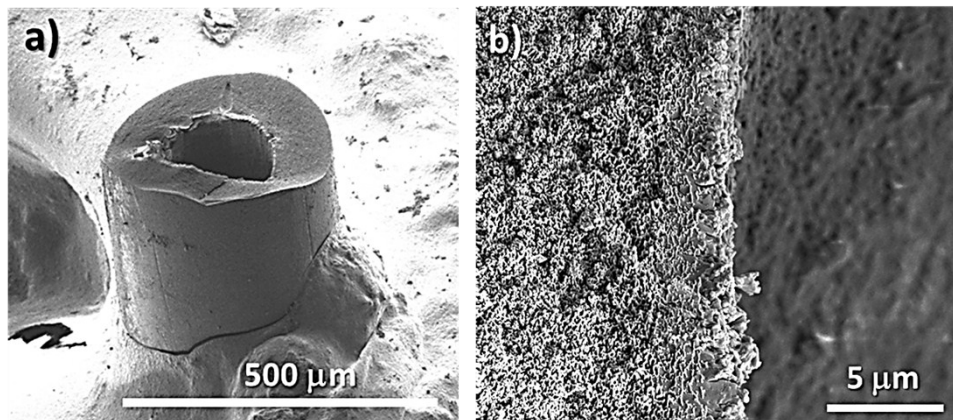
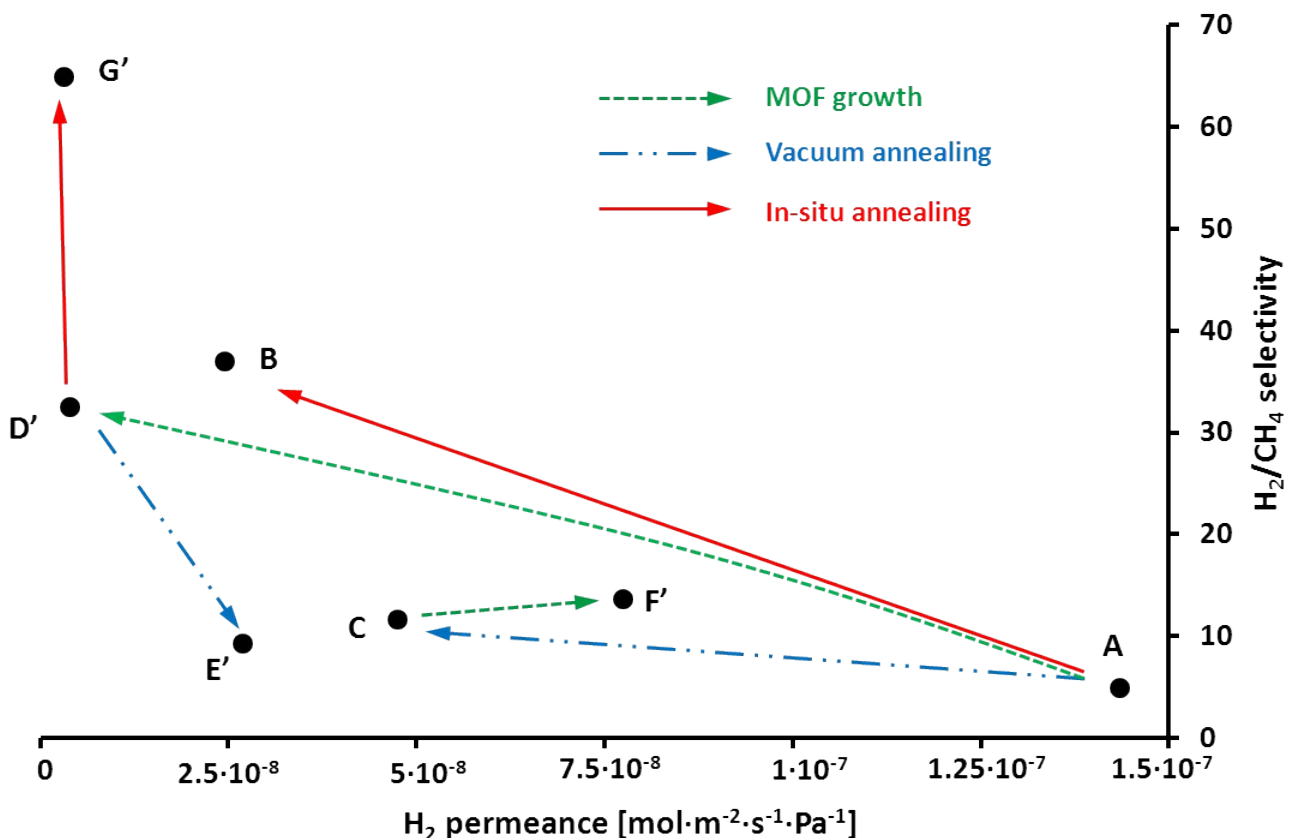


Figure S9. SEM cross-section images of the MOF-coated inner surface of an as-synthesized ZIF-93@P84 membrane.



Description of the membrane	H_2 permeance		H_2/CH_4 selectivity	CO_2 permeance		CO_2/CH_4 selectivity
	$\text{mol}\cdot\text{m}^{-2}\cdot\text{s}^{-1}\cdot\text{Pa}^{-1}$	GPU		$\text{mol}\cdot\text{m}^{-2}\cdot\text{s}^{-1}\cdot\text{Pa}^{-1}$	GPU	
D' ZIF-93 @ P84 HF membrane	$3.9\cdot10^{-9}$	12	32.4	$1.0\cdot10^{-9}$	3.0	10.5
E' Vacuum annealed D' membrane	$2.7\cdot10^{-8}$	80	9.2	$5.8\cdot10^{-9}$	17	2.1
F' ZIF-93 @ C membrane	$7.7\cdot10^{-8}$	231	13.6	$2.9\cdot10^{-8}$	86	5.1
G' In situ annealed D' membrane	$3.3\cdot10^{-9}$	9.7	65.0	$6.7\cdot10^{-10}$	2.0	19.6

Figure S10. Performance values at 35 °C of the ZIF-93@P84 HF membranes placed in a selectivity/permeance diagram for H_2/CH_4 mixture separation. CO_2/CH_4 mixture separation performance is also shown in the table. Data from A, B and C-type HF (bare and annealed P84) are the same as in Table 1.

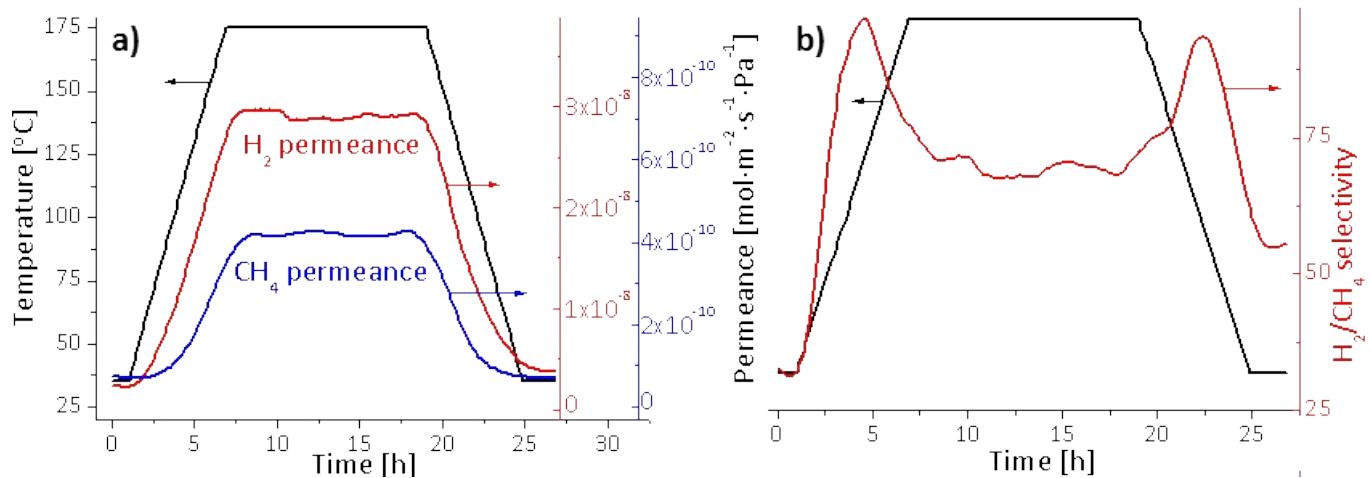


Figure S11. H_2 and CH_4 permeance and mixture selectivity dependence with time during *in situ* thermal annealing. A D'-type ZIF-93@P84 HF membrane was heated at 175 °C for 12 h with 6-h heating/cooling stages while separating a H_2/CH_4 gas mixture swept with Ar, resulting in a G'-type membrane.

Table S3. Extended data of HF membranes compared for H₂ purification. The performances obtained in this work are shown with those of other reported MOF-HF supported membranes, pure polyimide HFs and some CMSMs derived from them.

Ref.	MOF	HF support	T [°C]	H ₂ permeance [GPU]	Sel. H ₂ /CH ₄	Sel. H ₂ /CO ₂
4	ZIF-90	Torlon®	35	580	3.7	1.8
5	HKUST-1	PVDF	25	5884	5.4	8.1
6	ZIF-7	PVDF	Room	7031	20.3 (H ₂ /N ₂)	18.4
6	ZIF-8	PVDF	Room	6016	18.1 (H ₂ /N ₂)	16.3
7	HKUST-1	PSf/ PMDS	20	1449		21.0
8	HKUST-1	PAN	25	194743		7.1
9	ZIF-8	Torlon®	120	1090	328 (H ₂ /C ₃ H ₈)	
10	HKUST-1	PVDF	Room	17957		7.9
10	ZIF-8	PVDF	Room	5684		12.4
10	ZIF-7	PVDF	Room	3053		15.9
11	NH ₂ -MIL-53	PVDF	Room	16189		30.4
12	ZIF-7	PSf	35	7	34.6	2.4
12	ZIF-8	PSf	35	14	17.2	2.6
This work	ZIF-93	P84®	35	10	65.0	
	ZIF-8	P84®	35	39	72.4	
	ZIF-93	P84®	100	31	101.3	
	ZIF-8	P84®	100	104	103.1	
		P84®	35	429	4.9	
13,14		P84®	60	33	5.0	5.4
15	Matrimid® 5218		40	342	11.2	4.0
14	CMSMs from P84-HF		60	4	5732.6	20.9
13	CMSMs from P84-HF		60	8	843	14.9

ELECTRONIC SUPPLEMENTARY INFORMATION REFERENCES

1. O. Karvan, J. R. Johnson, P. J. Williams and W. J. Koros, *Chem. Eng. Technol.*, 2013, **36**, 53-61.
2. D. T. Clausi and W. J. Koros, *J. Membr. Sci.*, 2000, **167**, 79-89.
3. Y. Dai, J. R. Johnson, O. Karvan, D. S. Sholl and W. J. Koros, *J. Membr. Sci.*, 2012, **401–402**, 76-82.
4. A. J. Brown, J. R. Johnson, M. E. Lydon, W. J. Koros, C. W. Jones and S. Nair, *Angew. Chem. Int. Ed.*, 2012, **51**, 10615-10618.
5. Y. Mao, J. Li, W. Cao, Y. Ying, L. Sun and X. Peng, *ACS Appl. Mater. Interfaces*, 2014, **6**, 4473-4479.
6. W. Li, Q. Meng, X. Li, C. Zhang, Z. Fan and G. Zhang, *Chem. Commun.*, 2014, **50**, 9711-9713.
7. W. Li, G. Zhang, C. Zhang, Q. Meng, Z. Fan and C. Gao, *Chem. Commun.*, 2014, **50**, 3214-3216.
8. W. Li, Z. Yang, G. Zhang, Z. Fan, Q. Meng, C. Shen and C. Gao, *J. Mater. Chem. A*, 2014, **2**, 2110-2118.
9. A. J. Brown, N. A. Brunelli, K. Eum, F. Rashidi, J. R. Johnson, W. J. Koros, C. W. Jones and S. Nair, *Science*, 2014, **345**, 72-75.
10. W. Li, Q. Meng, C. Zhang and G. Zhang, *Chem. Eur. J.*, 2015, **21**, 7224-7230.
11. W. Li, P. Su, G. Zhang, C. Shen and Q. Meng, *J. Membr. Sci.*, 2015, **495**, 384-391.
12. F. Cacho-Bailo, S. Catalán-Aguirre, M. Etxeberria-Benavides, O. Karvan, V. Sebastian, C. Téllez and J. Coronas, *J. Membr. Sci.*, 2015, **476**, 277-285.
13. E. P. Favvas, E. P. Kouvelos, G. E. Romanos, G. I. Pilatos, A. C. Mitropoulos and N. K. Kanellopoulos, *J. Porous Mater.*, 2008, **15**, 625-633.
14. E. P. Favvas, N. S. Heliopoulos, S. K. Papageorgiou, A. C. Mitropoulos, G. C. Kapantaidakis and N. K. Kanellopoulos, *Sep. Purif. Technol.*, 2015, **142**, 176-181.
15. E. P. Favvas, G. C. Kapantaidakis, J. W. Nolan, A. C. Mitropoulos and N. K. Kanellopoulos, *J. Mater. Process. Technol.*, 2007, **186**, 102-110.